

**Topological and magnetic regulation in three cobalt(II)
coordination polymers constructed by mixed bipyrimidine-
tetracarboxylate strategy**

Zhengfang Tian, Shun-Yi Yang, Junlun Zhu, Zhijun Ruan, and Dong Shao*

Hubei Key Laboratory of Processing and Application of Catalytic Materials, College of
Chemistry and Chemical Engineering, Huanggang Normal University, Huanggang
438000, P. R. China

Email: shaodong@nju.edu.cn

Table of Contents

| | |
|--|----|
| EXPERIMENTAL SECTION | 3 |
| Figure S1. The asymmetric unit of compound 1 | 5 |
| Figure S2. The asymmetric unit of compound 2 | 5 |
| Figure S3. The asymmetric unit of compound 3 | 5 |
| Table S1. Selected bond lengths (Å) in 1 | 6 |
| Table S2. Selected bond lengths (Å) in 1 | 6 |
| Table S3. Continuous Shape Measure (CSHM) analysis for 1-3 | 7 |
| Table S4. Selected bond lengths (Å) in 2 | 8 |
| Table S5. Selected bond angles (Å) in 2 | 8 |
| Table S6. Selected bond lengths (Å) in 3 | 9 |
| Table S7. Selected bond angles (Å) in 3 | 9 |
| Figure S4. Portion of the widely H bonds in the structure of 1 | 10 |
| Figure S5. Comparison of the experimental and calculated PXRD patterns of 1 | 10 |
| Figure S6. Comparison of the experimental and calculated PXRD patterns of 2 | 11 |
| Figure S7. Comparison of the experimental and calculated PXRD patterns of 3 | 11 |
| Figure S8. The TGA curve of complex 1 | 12 |
| Figure S9. The TGA curve of complex 2 | 12 |
| Figure S10. The TGA curve of complex 3 | 12 |
| Figure S11. Temperature-dependent magnetic susceptibility for 3 . The red solid line represents the best fits by Curie-Weiss model. | 13 |
| Figure S12. Field dependence of the magnetization for 3 measured at 1.8 K. | 13 |
| Figure S13. Field-cooled magnetizations and zero-field-cooled magnetizations for 3 | 14 |
| Figure S14. Magnetization hysteresis loop for 3 measured at 1.8 K..... | 14 |
| Figure S15. Frequency dependence of the in-phase and out-of-phase ac susceptibilities measured under 0 Oe dc field for 2 | 15 |
| Figure S16. Frequency dependence of the in-phase and out-of-phase ac susceptibilities measured under 0 Oe dc field for 3 | 15 |
| Figure S17. Temperature dependence of the ac susceptibilities measured under 1 kOe dc field for 2 | 16 |
| Figure S18. Frequency dependence of the in-phase ac susceptibilities measured under 1 kOe dc field for 2 | 16 |
| Figure S19. Temperature dependence of the ac susceptibilities measured under 1 kOe dc field for 3 | 17 |

| | |
|---|----|
| Figure S20. Frequency dependence of the ac susceptibilities measured under 1 kOe dc field for 3 | 17 |
| Figure S21. Cole-Cole plots of 3 obtained from 1 kOe dc field..... | 18 |
| Figure S22. $\ln(\tau)$ vs T^{-1} plot for 3 . The red line represents the fit via Orbach mechanism. ... | 18 |
| Table S8. Relaxation fitting parameters from the least-square fitting of the Cole-Cole plots of 2 under 1 kOe dc field according to the generalized Debye model..... | 19 |
| Table S9. Relaxation fitting parameters from the least-square fitting of the Cole-Cole plots of 3 under 1 kOe dc field according to the generalized Debye model..... | 19 |
| References | 20 |

EXPERIMENTAL SECTION

Physical measurements

Elemental analyses of C, H, and N were performed at an Elementar Vario MICRO analyzer. Infrared spectra were obtained in the range of 600–4000 cm^{-1} on a Bruker tensor II spectrometer. Powder X-ray diffraction data (PXRD) were recorded on a Bruker D8 Advance diffractometer with Cu $K\alpha$ X-ray source ($\lambda = 1.54056 \text{ \AA}$) operated at 40 kV and 40 mA between 5 and 35° (2θ). Simulated PXRD patterns were obtained from the Mercury software. Thermal gravimetric analysis (TGA) was carried out on freshly filtered crystals using the Mettler Toledo TGA2 instrument in an insert Ar atmosphere over a temperature range of 30–600 °C with a heating rate of 10 °C/min.

Magnetic measurements

Direct current (DC) magnetic susceptibility from 2 to 300 K with applied 1000 Oe dc field were performed using a Quantum Design SQUID VSM magnetometer on the crushed single crystals sample of **1-3**. Alternative current (AC) magnetic susceptibility data were collected in a zero-dc field or an applied 1000 Oe dc fields in the

temperature range of 2-8 K, under an ac field of 2 Oe, oscillating at frequencies in the range of 1-1000 Hz. All magnetic data were corrected for the diamagnetic contributions of the sample holder and of core diamagnetism of the sample using Pascal's constants.

X-ray Crystallography

Single crystal X-ray diffraction data were collected on a Bruker D8 QUEST diffractometer with a PHOTON III area detector (Mo-K α radiation, $\lambda = 0.71073 \text{ \AA}$, Bruker *ius* 3.0) at room temperature. The APEX III program was used to determine the unit cell parameters and for data collection. The data were integrated and corrected for Lorentz and polarization effects using SAINT.^{S1} Absorption corrections were applied with SADABS.^{S2} The structures were solved by direct methods and refined by full-matrix least-squares method on F^2 using the SHELXTL^{S3} crystallographic software package integrated in Olex 2.^{S4} All the non-hydrogen atoms were refined anisotropically. Hydrogen atoms of the organic ligands were refined as riding on the corresponding non-hydrogen atoms. CCDC 2374155-2374157 are the supplementary crystallographic data for this paper. They can be obtained freely from the Cambridge Crystallographic Data Centre via www.ccdc.cam.ac.uk/data_request/cif.

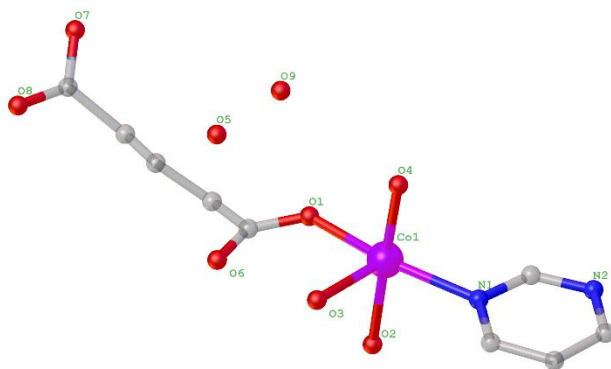


Figure S1. The asymmetric unit of compound 1.

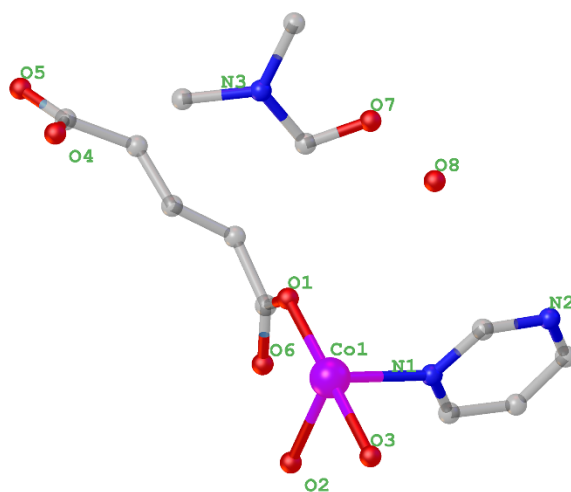


Figure S2. The asymmetric unit of compound 2.

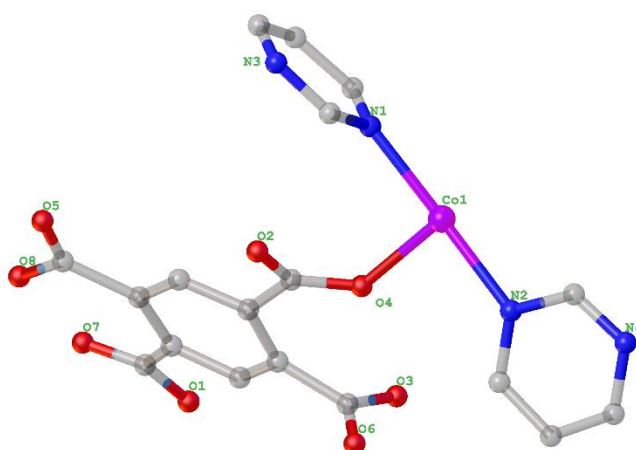


Figure S3. The asymmetric unit of compound 3.

Table S1. Selected bond lengths (Å) in **1**.

| | |
|--|------------|
| Co1-O1 | 2.0504(16) |
| Co1-O2 | 2.0988(19) |
| Co1- O3 | 2.0797(19) |
| Co1- O4 | 2.045(2) |
| Co1-N1 | 2.159(2) |
| Co1-N2 ¹ | 2.176(2) |
| Co-N/O _{average} | 2.101 |
| Symmetry operation: ¹ 1-X,1-Y,2-Z; ² 2-X,1-Y,1-Z | |

Table S2. Selected bond lengths (Å) in **1**.

| | |
|--|-----------|
| O1-Co1-O2 | 88.77(7) |
| O1-Co1-O3 | 89.21(7) |
| O1-Co1-N1 | 165.51(8) |
| O1-Co1-N2 ¹ | 89.78(7) |
| O2-Co1-N1 | 88.12(7) |
| O2-Co1-N2 ¹ | 95.24(8) |
| O3-Co1-O2 | 87.29(9) |
| O3-Co1-N1 | 104.77(8) |
| O3-Co1-N2 ¹ | 177.26(9) |
| O2-Co1-N3 | 96.36(9) |
| O4-Co1-O2 | 172.82(9) |
| Symmetry operation: ¹ 1-X,1-Y,2-Z; ² 2-X,1-Y,1-Z | |

Table S3. Continuous Shape Measure (CShM) analysis for **1-3**.

| Compound | CSM parameters* | | | | | Determined coordination geometry |
|----------|-------------------------------------|--------|--------------|--------|--------|----------------------------------|
| | six-coordinated coordination sphere | | | | | |
| | HP-6 | PPY-6 | OC-6 | TPR-6 | JPPY-6 | |
| 1 | 30.909 | 24.709 | 0.917 | 11.689 | 28.217 | OC-6 |
| 2 | 31.689 | 25.488 | 0.570 | 13.407 | 29.300 | |
| 3 | 29.045 | 22.733 | 1.161 | 12.124 | 26.358 | |

* CShM parameters for six-coordinated complexes:

HP-6 the parameter related to the hexagon (D_{6h})

PPY-6 the parameter related to the pentagonal pyramid (C_{5v})

OC-6 the parameter related to the octahedron (O_h)

TPR-6 the parameter related to the trigonal prism (D_{3h})

JPPY-6 the parameter related to the Johnson pentagonal pyramid (C_{5v})

Table S4. Selected bond lengths (Å) in **2**.

| | |
|---|----------|
| Co1-O1 | 2.074(2) |
| Co1-O2 | 2.091(2) |
| Co1- O3 | 2.098(2) |
| Co1- O4 ¹ | 2.067(2) |
| Co1-N1 | 2.170(3) |
| Co1-N2 ² | 2.180(3) |
| Co-N/O _{average} | 2.113 |
| Symmetry operation: ¹ -X,1-Y,1-Z; ² 1-X,1-Y,1-Z; ³ -X,1-Y,-Z | |

Table S5. Selected bond angles (°) in **2**.

| | |
|---|------------|
| O1-Co1-O2 | 91.58(9) |
| O1-Co1-O3 | 177.93(9) |
| O1-Co1-N1 | 88.68(9) |
| O1-Co1-N2 ¹ | 91.89(9) |
| O2-Co1-O3 | 89.54(9) |
| O2-Co1-N2 ¹ | 165.82(9) |
| O3-Co1-N1 | 93.06(9) |
| O3-Co1-N2 ¹ | 87.44(9) |
| O4 ² -Co1-N1 | 172.28(10) |
| O4 ² -Co1-N2 ¹ | 96.96(10) |
| N1-Co1-N2 ¹ | 76.08(9) |
| Symmetry operation: ¹ -X,1-Y,1-Z; ² 1-X,1-Y,1-Z; ³ -X,1-Y,-Z | |

Table S6. Selected bond lengths (Å) in **3**.

| | |
|--|----------|
| Co1-O1 ¹ | 2.044(2) |
| Co1-O4 | 2.016(2) |
| Co1-N1 | 2.122(2) |
| Co1-N2 | 2.115(2) |
| Co1-N3 ² | 2.151(2) |
| Co1-N4 ³ | 2.165(2) |
| Co-N/O _{average} | 2.102 |
| Symmetry operation: ¹ 1-X,1-Y,1-Z; ² 2-X,2-Y,2-Z; ³ 2-X,1-Y,2-Z | |

Table S7. Selected bond angles (°) in **3**.

| | |
|--|-----------|
| O1 ¹ -Co1-N1 | 89.26(9) |
| O1-Co1-N2 | 96.65(9) |
| O1-Co1-N3 ² | 164.72(9) |
| O4-Co1-O1 ¹ | 92.20(9) |
| O4-Co1-N1 | 90.33(9) |
| O4-Co1-N2 | 91.10(9) |
| O4-Co1-N4 ³ | 168.54(9) |
| N1-Co1-N3 ² | 78.05(9) |
| N1-Co1-N4 ³ | 100.22(9) |
| N2-Co1-N1 | 173.86(9) |
| N2-Co1-N3 ² | 95.86(9) |
| Symmetry operation: ¹ 1-X,1-Y,1-Z; ² 2-X,2-Y,2-Z; ³ 2-X,1-Y,2-Z | |

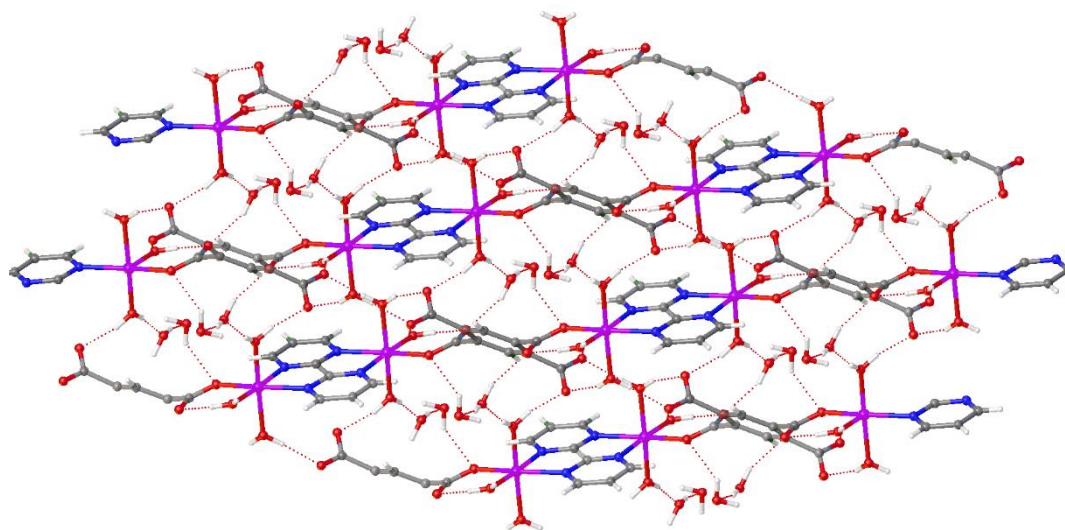


Figure S4. Portion of the widely H bonds in the structure of **1**.

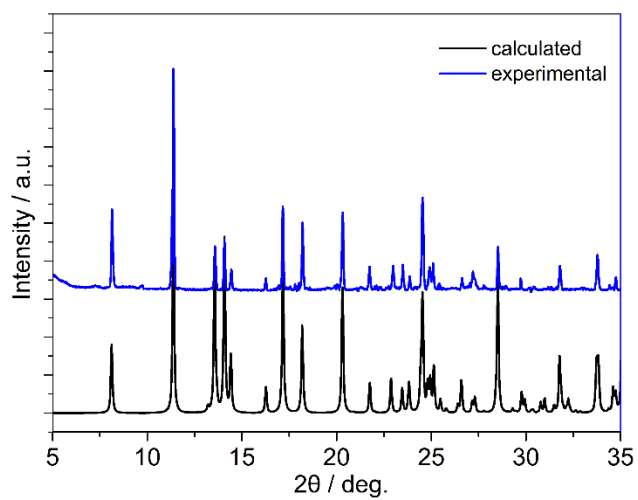


Figure S5. Comparison of the experimental and calculated PXRD patterns of **1**.

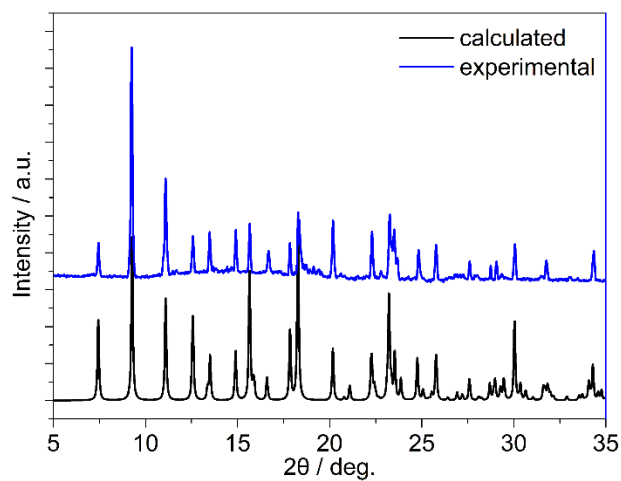


Figure S6. Comparison of the experimental and calculated PXRD patterns of **2**.

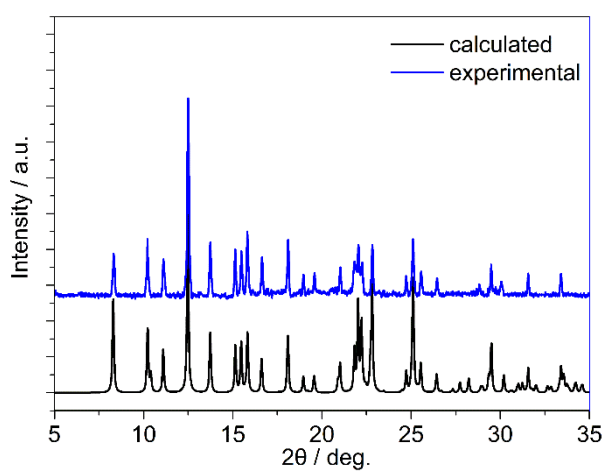


Figure S7. Comparison of the experimental and calculated PXRD patterns of **3**.

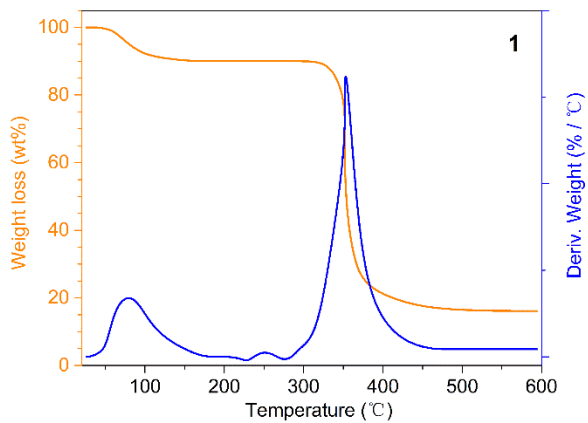


Figure S8. The TGA curve of complex 1

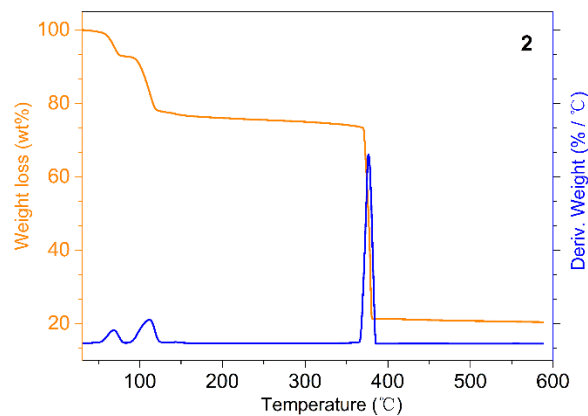


Figure S9. The TGA curve of complex 2.

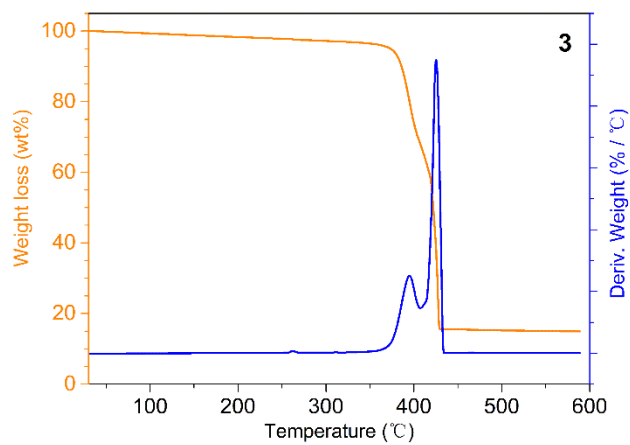


Figure S10. The TGA curve of complex 3.

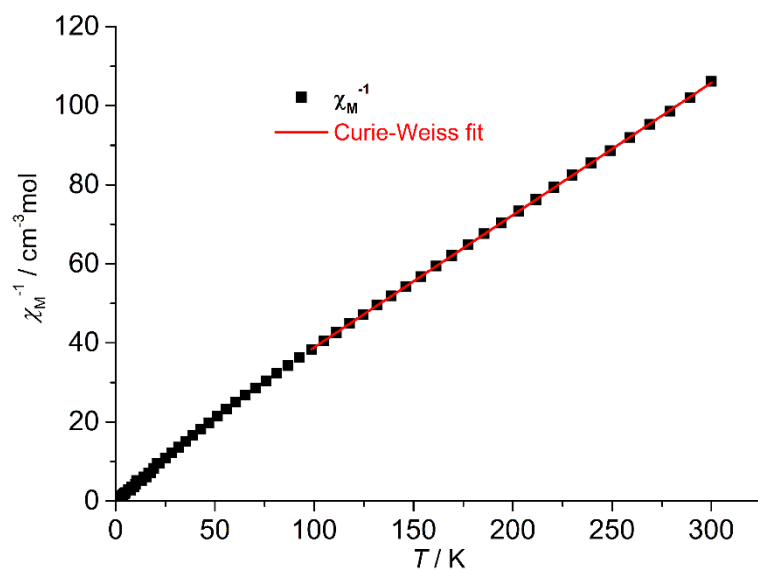


Figure S11. Temperature-dependent magnetic susceptibility for **3**. The red solid line represents the best fits by Curie-Weiss model.

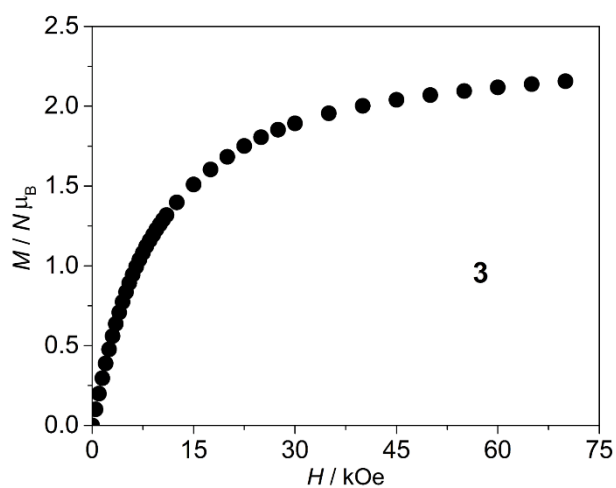


Figure S12. Field dependence of the magnetization for **3** measured at 1.8 K.

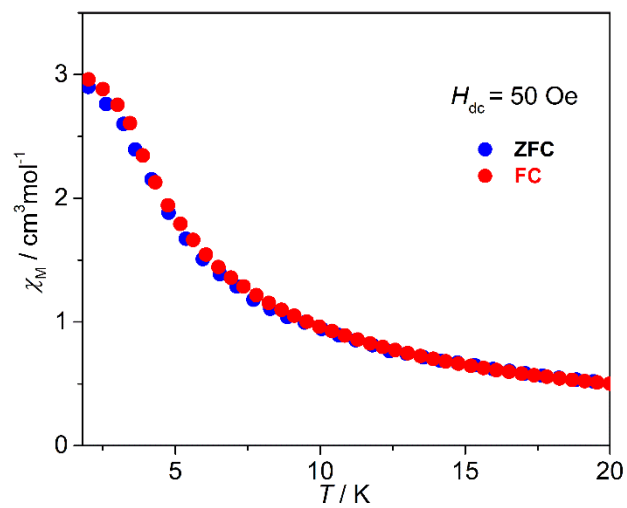


Figure S13. Field-cooled magnetizations and zero-field-cooled magnetizations for **3**.

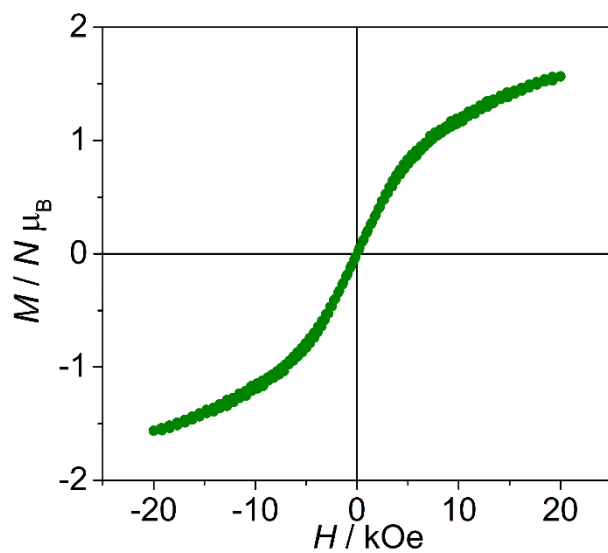


Figure S14. Magnetization hysteresis loop for **3** measured at 1.8 K.

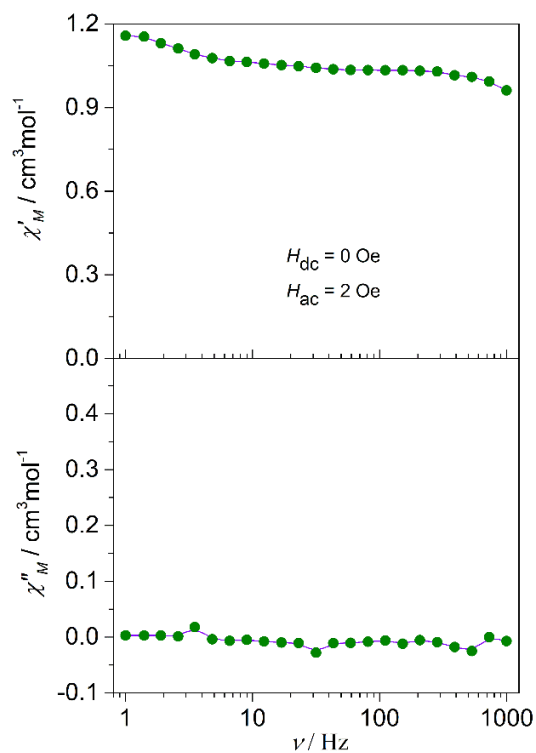


Figure S15. Frequency dependence of the in-phase and out-of-phase ac susceptibilities measured under 0 Oe dc field for **2**.

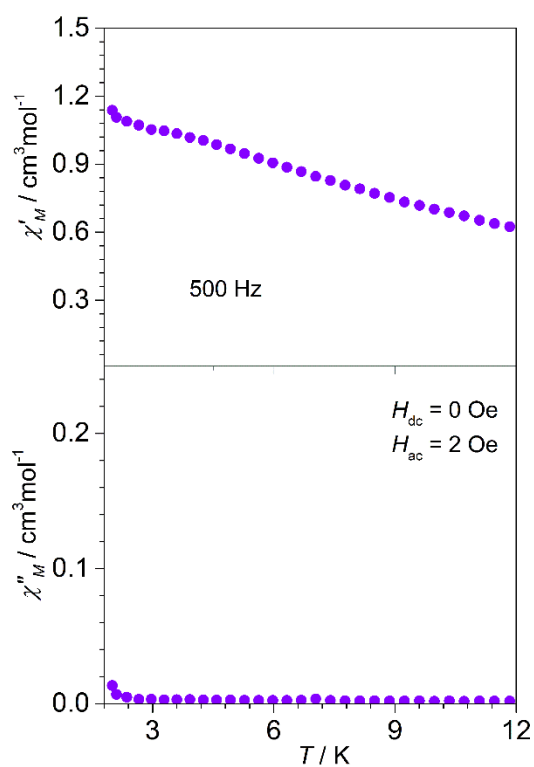


Figure S16. Frequency dependence of the in-phase and out-of-phase ac susceptibilities measured under 0 Oe dc field for **3**.

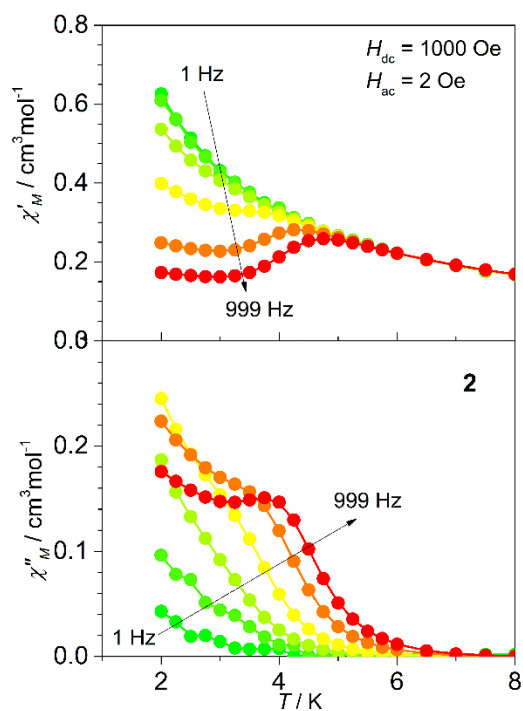


Figure S17. Temperature dependence of the ac susceptibilities measured under 1 kOe dc field for **2**.

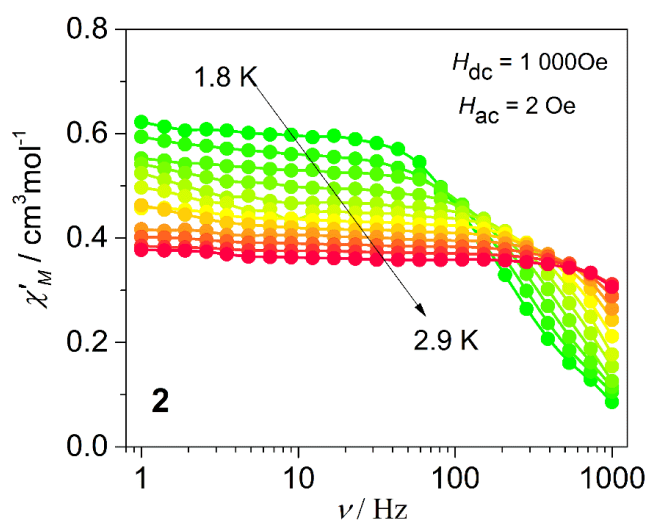


Figure S18. Frequency dependence of the in-phase ac susceptibilities measured under 1 kOe dc field for **2**.

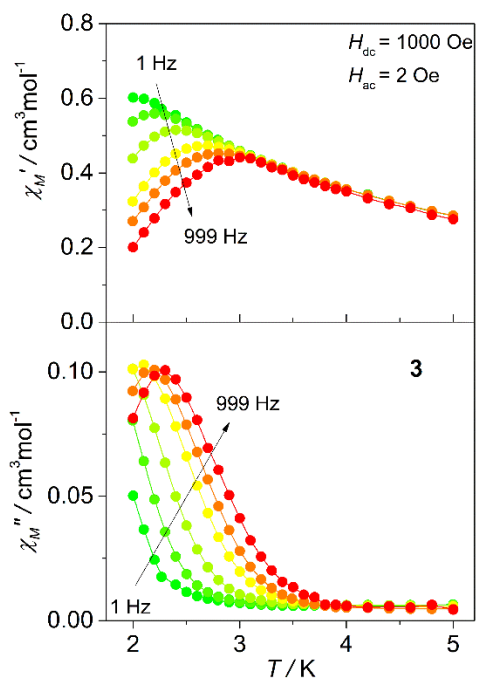


Figure S19. Temperature dependence of the ac susceptibilities measured under 1 kOe dc field for **3**.

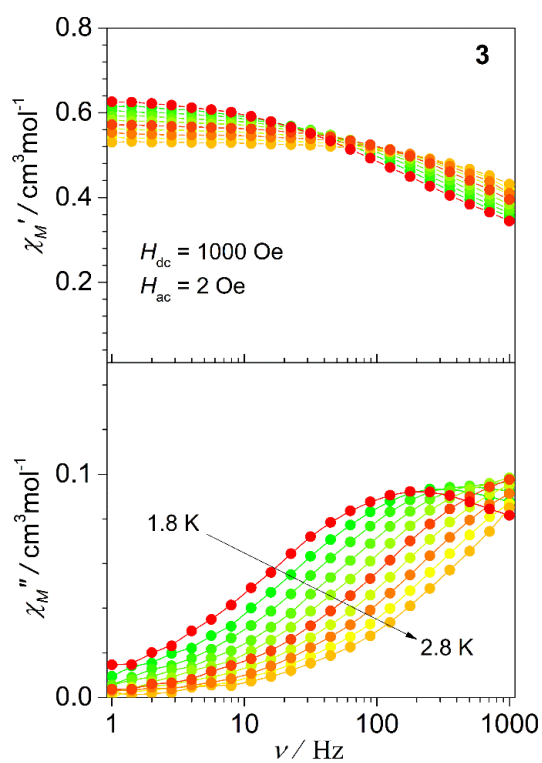


Figure S20. Frequency dependence of the ac susceptibilities measured under 1 kOe dc field for **3**.

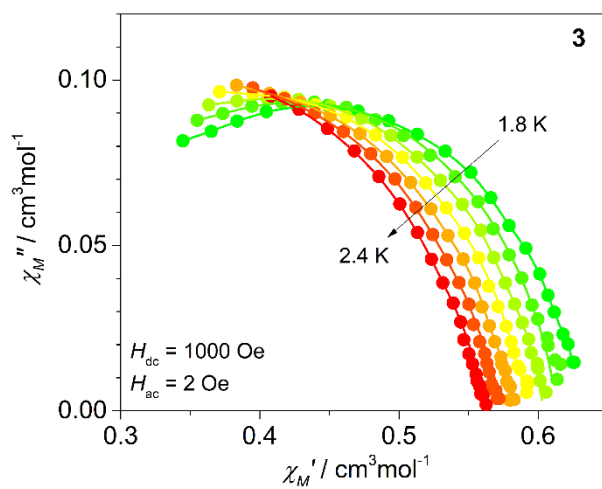


Figure S21. Cole-Cole plots of **3** obtained from 1 kOe dc field.

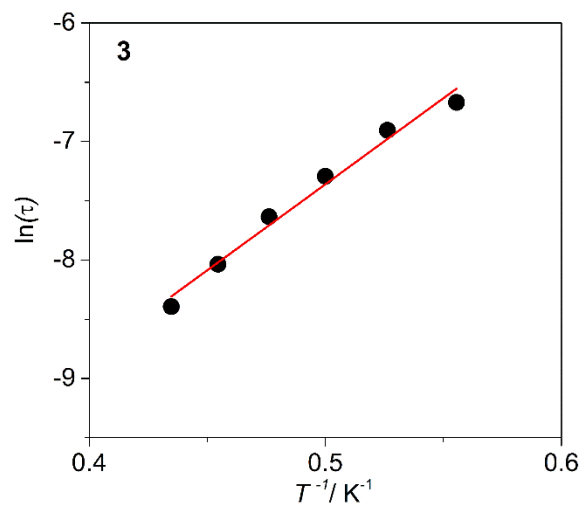


Figure S22. $\ln(\tau)$ vs T^{-1} plot for **3**. The red line represents the fit via Orbach mechanism.

Table S8. Relaxation fitting parameters from the least-square fitting of the Cole-Cole plots of **2** under 1 kOe dc filed according to the generalized Debye model.

| T / K | τ / s | χ_S / cm ³ mol ⁻¹ K | χ_T / cm ³ mol ⁻¹ K | α |
|-------|------------|--|--|----------|
| 1.8 | 0.0012 | 0.065 | 0.651 | 0.117 |
| 1.9 | 1E-3 | 0.068 | 0.631 | 0.108 |
| 2 | 7.6E-4 | 0.089 | 0.581 | 0.045 |
| 2.1 | 5.6E-4 | 0.049 | 0.565 | 0.091 |
| 2.2 | 4.3E-4 | 0.020 | 0.538 | 0.111 |
| 2.3 | 3.4E-4 | 0.024 | 0.515 | 0.145 |
| 2.4 | 2.8E-4 | 0.052 | 0.492 | 0.143 |
| 2.5 | 2.3E-4 | 0.073 | 0.471 | 0.148 |

Table S9. Relaxation fitting parameters from the least-square fitting of the Cole-Cole plots of **3** under 1 kOe dc filed according to the generalized Debye model.

| T / K | τ / s | χ_S / cm ³ mol ⁻¹ K | χ_T / cm ³ mol ⁻¹ K | α |
|-------|------------|--|--|----------|
| 1.8 | 0.001 | 0.014 | 0.657 | 0.123 |
| 1.9 | 0.001 | 0.012 | 0.642 | 0.211 |
| 2 | 8.8E-4 | 0.011 | 0.623 | 0.152 |
| 2.1 | 6.3E-4 | 0.012 | 0.611 | 0.231 |
| 2.2 | 4.2E-4 | 0.01 | 0.604 | 0.216 |
| 2.3 | 2.9E-4 | 0.012 | 0.585 | 0.124 |

References

- S1) SAINT Software Users Guide, version 7.0; Bruker Analytical X-Ray Systems: Madison, WI, 1999.
- S2) G. M. Sheldrick, SADABS, version 2.03; Bruker Analytical X-Ray Systems, Madison, WI, 2000.
- S3) G. M. Sheldrick, SHELXTL, Version 6.14, Bruker AXS, Inc.; Madison, WI 2000-2003.
- S4) O. V. Dolomanov, L. J. Bourhis, R. J. Gildea, J. A. K. Howard, H. Puschmann, OLEX2: A Complete Structure Solution, Refinement and Analysis Program. *J. Appl. Crystallogr.*, 2009, 42, 339–341.